

F-Doped Co_3O_4 Photocatalysts for Sustainable H_2 Generation from Water/Ethanol

Alberto Gasparotto,^{*,†} Davide Barreca,[§] Daniela Bekermann,[†] Anjana Devi,^{||} Roland A. Fischer,^{||} Paolo Fornasiero,^{*,‡} Valentina Gombac,[‡] Oleg I. Lebedev,[#] Chiara Maccato,[†] Tiziano Montini,[‡] Gustaaf Van Tendeloo,[⊥] and Eugenio Tondello[†]

[†]Department of Chemistry, Padova University and INSTM, via Marzolo 1, 35131 Padova, Italy

[§]CNR-ISTM and INSTM, Department of Chemistry, Padova University, via Marzolo 1, 35131 Padova, Italy

^{||}Lehrstuhl für Anorganische Chemie II, Ruhr-University Bochum, Universitätsstrasse 150, 44780 Bochum, Germany

[‡]Department of Chemical and Pharmaceutical Sciences, ICCOM-CNR Trieste Research Unit, INSTM Trieste Research Unit, Trieste University, via L. Giorgieri 1, 34127 Trieste, Italy

[#]Laboratoire CRISMAT, UMR 6508, CNRS-ENSICAEN, Bd. Maréchal Juin 6, 14050 Caen Cedex 4, France

[⊥]EMAT, Antwerp University, Groenenborgerlaan 171, 2020 Antwerp, Belgium

S Supporting Information

ABSTRACT: p-Type Co_3O_4 nanostructured films are synthesized by a plasma-assisted process and tested in the photocatalytic production of H_2 from water/ethanol solutions under both near-UV and solar irradiation. It is demonstrated that the introduction of fluorine into p-type Co_3O_4 results in a remarkable performance improvement with respect to the corresponding undoped oxide, highlighting F-doped Co_3O_4 films as highly promising systems for hydrogen generation. Notably, the obtained yields were among the best ever reported for similar semiconductor-based photocatalytic processes.

Photocatalytic production of H_2 from water-containing solutions is a fascinating scientific and technological challenge to store radiant energy in molecular hydrogen.^{1–4} In this field, a great deal of effort has been devoted to the design and development of n-type semiconducting photocatalysts, such as TiO_2 and ZnO , and their chemical modification aimed at obtaining improved functional properties.^{2,3,5–8} In particular, anion doping of the oxide phase has attracted considerable interest for the possibility of achieving optimal solar light absorption and enhanced surface reactivity, along with efficient exploitation of photogenerated electron/hole (e^-/h^+) pairs.^{1,7–15} Nevertheless, although anion doping has been widely studied for n-type semiconductors (SCs), its potential has been scarcely investigated for photocatalytic processes over p-type materials and never reported for photoassisted H_2 production. To this aim, although autothermal reforming of alcohols and aqueous phase reforming are considered promising mid-term solutions due to their high efficiency,¹⁶ light-activated catalytic processes have recently emerged as more sustainable long-term alternatives for energy production.^{2,3,4b,4c}

In contrast to n-type SCs, in p-type systems cation vacancies and/or anion interstitials are considered the main kind of intrinsic defects. As a consequence, a different surface reactivity can be foreseen upon reactant adsorption on the catalyst surface.^{17,18}

Furthermore, the presence of sub-surface defects in p-type SCs, acting either as recombination centers or as beneficial promoters of redox processes, might also affect the fate of photogenerated electrons and holes.^{2,11,17} To this aim, extrinsic anion doping of SCs represents a valuable way to obtain improved photocatalytic performances. In order to make feasible the dream of utilizing sunlight for sustainable energy production, it is of paramount importance to develop catalytic systems that are not affected by leaching or poisoning phenomena and possess a high photonic efficiency, in particular upon visible activation. Recently we have reported that Co_3O_4 , a multifunctional spinel-type p-type SC,^{18–20} is capable of promoting hydrogen photoproduction in the presence of methanol as sacrificial agent.^{4a} This material, however, suffered rapid deactivation due to the surface formation of inactive CoO species and the adsorption of intermediates arising from methanol partial oxidation. The presence of oxygen ($\sim 9 \text{ mg L}^{-1}$) resulted in improved photocatalytic performance.

Herein, we report on a versatile one-step synthesis of F-doped Co_3O_4 and on the considerable H_2 photoproduction enhancement arising from anion doping with respect to the bare oxide phase. In this case, ethanol was used as sacrificial agent, as it is more sustainable and renewable than methanol.

Undoped and F-doped Co_3O_4 nanostructured films were synthesized via plasma enhanced chemical vapor deposition (PE-CVD) from both fluorine-free and fluorinated β -diketonate cobalt derivatives [$\text{Co}(\text{dpm})_2$] and [$\text{Co}(\text{hfa})_2\text{TMEDA}$], respectively (see the Supporting Information (SI)). As evidenced by electron impact mass spectrometry (EI-MS) data, in the latter case the elimination of fluorine radicals and the formation of several F-containing species took place (Figure S2). Since the ionization conditions used for EI-MS analyses are analogous to those adopted in PE-CVD processes, it is reasonable to suppose that a similar fragmentation pathway also occurred during the plasma-assisted growth of Co_3O_4 -based systems, thus explaining the effective fluorine incorporation into the deposited materials.

Received: October 26, 2011

Published: November 04, 2011

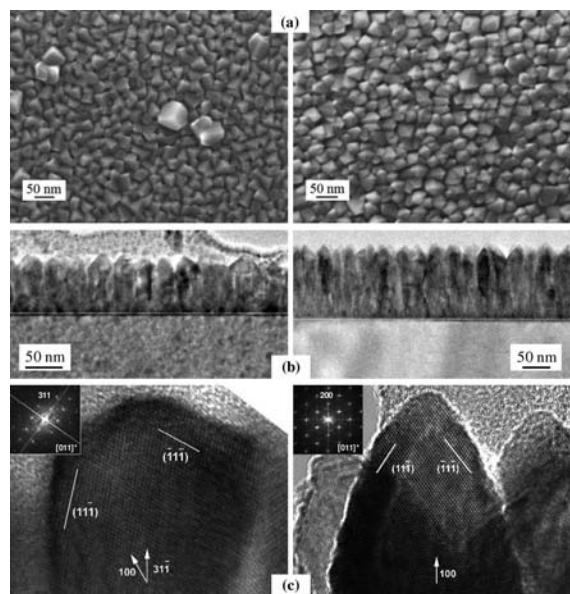


Figure 1. (a) Plane-view FE-SEM, (b) cross-sectional TEM, and (c) HRTEM images of undoped (left) and F-doped (right) Co_3O_4 samples. FT patterns of the HRTEM images are given as insets in (c).

This hypothesis was confirmed by X-ray photoelectron spectroscopy (XPS), evidencing a homogeneous in-depth fluorine distribution for samples synthesized from $[\text{Co}(\text{hfa})_2\text{TMEDA}]$ (see below).

Figure 1a displays plane-view field emission scanning electron microscopy (FE-SEM) images of an undoped Co_3O_4 sample (left) and the corresponding F-doped specimen (right) synthesized under the same growth conditions. In both cases, the surface texture was dominated by pyramidal-like aggregates with a mean lateral size of 30 nm that, according to transmission electron microscopy (TEM) cross-sectional analyses (Figure 1b), represented the tip of columnar structures grown perpendicular to the Si(100) substrate (deposit thickness = 80–90 nm). Irrespective of the precursor used and the processing conditions adopted, electron diffraction (ED) patterns (not reported) were always characterized by the sole reflections expected for spinel-type Co_3O_4 . No appreciable ED variation was observed upon F-doping, a result traced back to the similar radii of fluorine and oxygen and to the substitutional fluorine doping of the spinel phase.^{11,12} High resolution TEM (HRTEM) and Fourier transform (FT) analyses (Figure 1c) showed that the growth directions of the columnar structures displayed in Figure 1b were generally the $\langle 311 \rangle$ and $\langle 100 \rangle$ ones for undoped and doped Co_3O_4 , respectively. Nevertheless, in both cases, $\{111\}$ surface planes, the most stable for face-centered cubic systems such as Co_3O_4 , were preferentially exposed.^{4a,21} This feature, in line with the pyramidal-like morphology of undoped and F-doped Co_3O_4 (Figure 1a), highlights that their diverse photocatalytic activities (see below) cannot be related to exposure of facets with different Miller indexes.^{19,20}

In an attempt to clarify this issue, XPS analyses were performed, providing valuable compositional information. In line with our previous work,^{4a,21,22} the shape and position of surface Co2p and CoLMM photopeaks (data not shown) clearly indicated the formation of Co_3O_4 -based systems, irrespective of the precursor used. Nevertheless, whereas for samples synthesized from $[\text{Co}(\text{dpm})_2]$ in-depth analyses evidenced a parallel distribution of the sole Co and O signals (Figure 2a, left), the

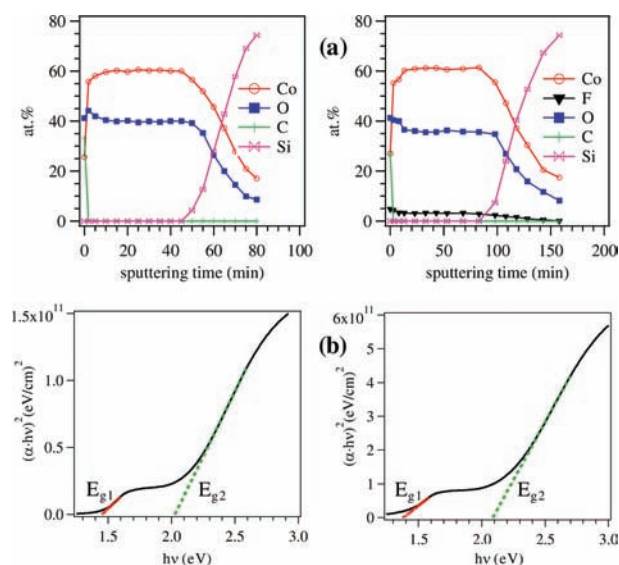


Figure 2. (a) XPS depth profiles and (b) Tauc plots of undoped (left) and F-doped (right) Co_3O_4 specimens.

use of $[\text{Co}(\text{hfa})_2\text{TMEDA}]$ also resulted in a constant fluorine content (~ 3 atom%) from the surface to the interface with the substrate (Figure 2a, right). As better described in the SI (see Figure S3), such a result indicated homogeneous fluorine incorporation in the oxide lattice and the obtaining of F-doped Co_3O_4 nanodeposits. XPS investigation also highlighted the sudden disappearance of the carbon signal upon erosion, demonstrating clean precursor decomposition under the adopted PE-CVD conditions and the high purity of the obtained systems.

In order to elucidate the impact of fluorine doping on the material's optical properties, UV–vis absorption measurements were performed. Band-gap estimation from the Tauc plots of Figure 2b yielded values of 1.4–1.5 (E_{g1}) and 2.0–2.1 eV (E_{g2}) for both undoped and doped systems, indicating a negligible influence of fluorine doping.²² The optical absorption in the visible range demonstrated that Co_3O_4 -based materials are promising SCs for the photocatalytic utilization of solar energy.^{23,24} Interestingly, a comparison of the Tauc plots reported in Figure 2b clearly revealed a 2-fold increase of the absorption coefficient for F-doped Co_3O_4 , an important goal for efficient light harvesting and subsequent exploitation of e^-/h^+ pairs.^{24,25} In fact, since the diffusion length of charge carriers in SC oxides is small (typically a few nanometers), it is important that photons are largely absorbed in the near-surface layers, so that photo-generated e^- and h^+ species can effectively reach the catalyst surface and participate in the target chemical processes.

Photoassisted H_2 generation was carried out under both near-UV (125 W Hg lamp with a photon flux of 29 mW cm^{-2} at 360 nm, 100 mW cm^{-2} in the 400–1050 nm interval) and simulated sunlight irradiation (150 W Xe lamp, 180 mW cm^{-2}), using 1:1 water/ethanol solutions (see SI). No appreciable evolution of gaseous products was observed when illumination and photocatalyst (geometrical area = 3 cm^2) were not simultaneously present. Furthermore, only a weak and transient reactivity was revealed for deaerated water/ethanol solutions, due to the surface formation of inactive CoO, as previously reported for bare Co_3O_4 .^{4a}

Under near-UV irradiation and in the presence of O_2 (Figure 3a), undoped Co_3O_4 showed an average hydrogen production of $\sim 3 \mu\text{mol h}^{-1} \text{ cm}^{-2}$, whereas in the presence of

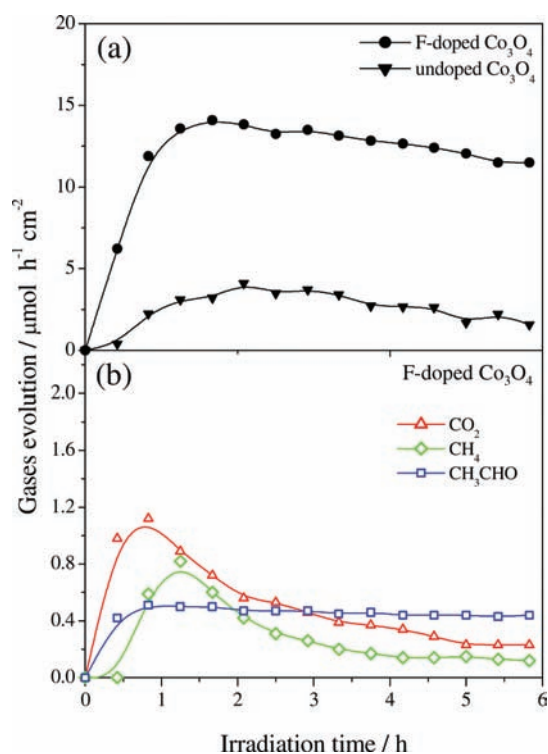


Figure 3. (a) H_2 evolution from a water/ethanol solution upon near-UV irradiation for undoped and fluorine-doped Co_3O_4 catalysts. (b) Evolution of C-containing gaseous products for the F-doped sample reported in (a).

fluorine the H_2 evolution rate was increased 5-fold. For the latter sample, an estimation of the catalyst amount based on film thickness and Co_3O_4 bulk density led to an activity of $213\,000\ \mu\text{mol h}^{-1} \text{g}^{-1}$ ($45\,000\ \mu\text{mol h}^{-1} \text{g}^{-1}$ for undoped Co_3O_4). Notably, this is one of the best values ever reported in the literature for SC-based photocatalytic hydrogen generation, also taking into account that no cocatalysts (e.g., Rh, Pd, Pt) were used in this work.²

The parallel evolution of CO_2 and CH_3CHO , resulting from ethanol oxidation, over F-doped Co_3O_4 (Figure 3b) suggested the occurrence of two concomitant reaction pathways involving adsorbed ethanol and liquid-phase reactions between $\text{CH}_3\text{CH}_2\text{OH}$ and free OH^\bullet , respectively.²⁶ The slight decrease of the H_2 yield and the net rate reduction for CO_2 and CH_4 could be associated mainly with CoO surface formation, attributed, in turn, to a progressive oxygen depletion in the reaction medium (see SI). Notably, acetaldehyde evolution was almost constant (Figure 3b), suggesting thus the establishment of a gas-liquid equilibrium ensuring a buffering condition. For liquid-phase products (see Figure S5), an interesting effect observed for F-doped Co_3O_4 was the photoassisted generation of 2,3-butanediol, a useful precursor for the industrial production of methyl ethyl ketone and 1,3-butadiene.^{27,28}

Figure 3a also displays the presence of an initial induction period (duration ~ 75 min) characterized by a progressive increase of the hydrogen evolution rate. This phenomenon suggests the occurrence of light-induced surface activation, followed by the establishment of an equilibrium between the byproducts adsorbed on the catalyst surface and in the liquid/gas phase.

The 5-fold increase of the hydrogen yield observed for the fluorinated catalyst can be explained by the synergistic combination of various beneficial phenomena. Specifically, it

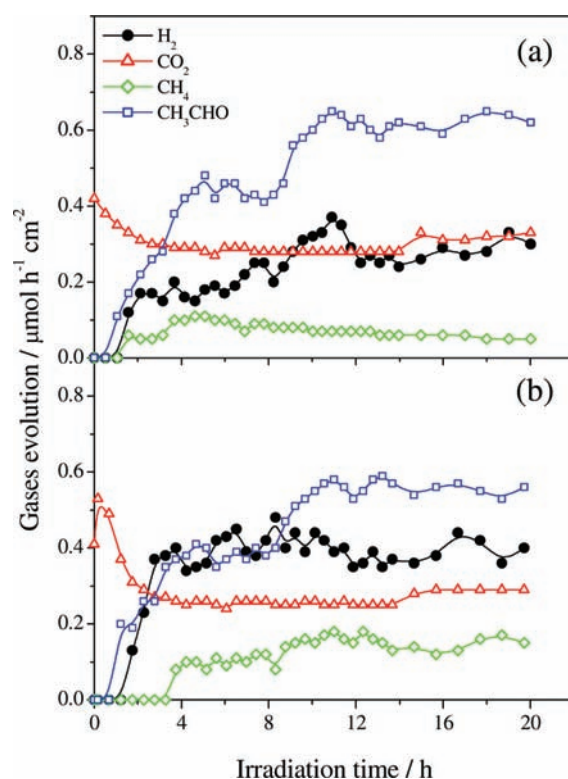


Figure 4. Evolution of gases from a water/ethanol solution upon simulated sunlight irradiation for undoped (a) and fluorine-doped (b) Co_3O_4 catalysts.

has been reported that replacement of surface $-\text{OH}$ groups by fluorine can lead to: (i) an increase of free OH^\bullet radicals in the liquid-phase, resulting in faster ethanol oxidation and concomitant enhancement of $\text{H}^+ \rightarrow \text{H}_2$ reduction;^{29,30} (ii) inhibition of e^-/h^+ recombination;³¹ and (iii) modification of absorption properties and/or tuning of band position.^{7,32} Since the presence of fluorine does not significantly change band-gap values (see above), the improved performance of F-doped Co_3O_4 could be mainly traced back to points (i) and (ii) and, in particular, to the larger availability of OH^\bullet radicals. In addition, F-doping could induce a favorable shift of Co_3O_4 flat-band potentials, rendering photogenerated electrons more available for hydrogen production.²³ Finally, the presence of fluorine on the catalyst surface might enhance the Lewis acidity of cobalt centers, as also observed for TiO_2 -based photocatalysts, beneficially affecting the system activity.^{7,11,13}

At variance with the case of UV illumination (Figure 3), use of the less energetic simulated sunlight (Figure 4) enabled us to perform photocatalytic experiments for 20 h of irradiation without significantly altering the water/ethanol molar ratio. In fact, variation in the concentration of sacrificial agent could affect hydrogen production.³³ Under these more sustainable conditions, a lower, though appreciable, hydrogen evolution was still observed (Figure 4). Compared to bare Co_3O_4 , the fluorinated specimen showed an almost 2-fold increase in H_2 production (corresponding to $6500\ \mu\text{mol h}^{-1} \text{g}^{-1}$), along with a slightly more abundant methane evolution, as a result of acetic acid degradation or CO_2 hydrogenation (see also Figure S6). The relatively high initial CO_2 evolution is in line with the presence of carbonate traces on the catalyst surface²¹ that are progressively decomposed under the present reaction conditions. Nevertheless,

after 2 h of irradiation, constant CO₂ production was observed, indicating the occurrence of ethanol photoreforming involving a C–C bond cleavage. Notably, at variance with the case of UV light, no appreciable decrease of the hydrogen evolution rate was revealed during simulated sunlight irradiation, even after 20 h of reaction. Such improved system stability was ascribed to several possible contributing effects. First, the lower conversion of ethanol into H₂ and other C-containing byproducts with respect to the case of Figure 3 implies lower surface coverage/poisoning by partially oxidized species. In addition, the lower H₂ yield minimizes the reaction between hydrogen and the oxygen present in solution, thus decreasing the formation of inactive CoO surface species.^{4a} As a final remark, it is relevant to observe that, in contrast to powdered photocatalysts, supported nanosystems allow the use of minimal amounts of material and reduce aggregation effects, thus resulting in an improved time stability.

In conclusion, F-doping of Co₃O₄ films synthesized by PE-CVD resulted in a significant improvement of H₂ photoproduction from suitable aqueous solutions. Specifically, upon near-UV irradiation of F-doped Co₃O₄, a 5-fold hydrogen yield increase was evidenced with respect to the corresponding undoped oxide. In the case of simulated solar light, although a less marked improvement in terms of H₂ evolution was observed, the appreciable time stability of the response makes this material an attractive photocatalyst for the sustainable generation of hydrogen activated by sunlight. As a whole, the incorporation of fluorine resulted in highly photoactive Co₃O₄ materials, with H₂ yields per gram of catalyst among the best ever reported in the literature.

It is also worth noting that the synthetic strategy adopted herein for the preparation of F-doped Co₃O₄ can be regarded as a general and versatile route for tailored anion doping of oxide and even non-oxide SC nanosystems. Efforts in this direction are currently underway.

■ ASSOCIATED CONTENT

S Supporting Information. Details on Co₃O₄ and F-doped Co₃O₄ nanodeposit preparation, characterization, and functional testing. This material is available free of charge via the Internet at <http://pubs.acs.org>.

■ AUTHOR INFORMATION

Corresponding Author

alberto.gasparotto@unipd.it; pforناسiero@units.it

■ ACKNOWLEDGMENT

This work was supported by funding from the European Community 7th Framework Program FP7/2007-2013 (grant agreement no. ENHANCE-238409). PRIN-COFIN 2008, Padova University PRAT 2010, Regione Lombardia-INSTM PICASSO, ALADIN Industria 2015, Regione Friuli Venezia Giulia (IDROBIM project), and Fondo Trieste have provided further financial support. Dr. Roberta Seraglia (CNR, Padova, Italy), Dr. Cinzia Sada (Padova University, Italy), and Dr. Marco Gavagnin (Vienna University of Technology, Austria) are acknowledged for technical assistance and experimental support.

■ REFERENCES

(1) Kim, H. G.; Hwang, D. W.; Lee, J. S. *J. Am. Chem. Soc.* **2004**, *126*, 8912.

- (2) Chen, X.; Shen, S.; Guo, L.; Mao, S. S. *Chem. Rev.* **2010**, *110*, 6503.
- (3) Abe, R. *J. Photochem. Photobiol., C* **2010**, *11*, 179.
- (4) (a) Barreca, D.; Fornasiero, P.; Gasparotto, A.; Gombac, V.; Maccato, C.; Pozza, A.; Tondello, E. *Chem. Vap. Deposition* **2010**, *16*, 296. (b) Barreca, D.; Carraro, G.; Gombac, V.; Gasparotto, A.; Maccato, C.; Fornasiero, P.; Tondello, E. *Adv. Funct. Mater.* **2011**, *21*, 2611. (c) Cargnello, M.; Gasparotto, A.; Gombac, V.; Montini, T.; Barreca, D.; Fornasiero, P. *Eur. J. Inorg. Chem.* **2011**, 4309.
- (5) Wang, J.; Tafen, D. N.; Lewis, J. P.; Hong, Z.; Manivannan, A.; Zhi, M.; Li, M.; Wu, N. *J. Am. Chem. Soc.* **2009**, *131*, 12290.
- (6) Shet, S.; Ahn, K.-S.; Nuggehalli, R.; Yan, Y.; Turner, J.; Al-Jassim, M. *Thin Solid Films* **2011**, *519*, 5983.
- (7) Sun, H.; Wang, S.; Ming Ang, H.; Tadé, O. M.; Li, Q. *Chem. Eng. J.* **2010**, *162*, 437.
- (8) Czoska, A. M.; Livraghi, S.; Chiesa, M.; Giamello, E.; Agnoli, S.; Granozzi, G.; Finazzi, E.; Di Valentin, C.; Pacchioni, G. *J. Phys. Chem. C* **2008**, *112*, 8951.
- (9) Liu, G.; Yang, H. G.; Wang, X.; Cheng, L.; Pan, J.; (Max) Lu, G. Q.; Cheng, H.-M. *J. Am. Chem. Soc.* **2009**, *131*, 12868.
- (10) Zuo, F.; Wang, L.; Wu, T.; Zhang, Z.; Borchardt, D.; Feng, P. *J. Am. Chem. Soc.* **2010**, *132*, 11856.
- (11) Chen, D.; Jiang, Z.; Geng, J.; Zhu, J.; Yang, D. *J. Nanopart. Res.* **2009**, *11*, 303.
- (12) Xu, J.; Ao, Y.; Fu, D.; Yuan, C. *Appl. Surf. Sci.* **2008**, *254*, 3033.
- (13) Zhao, Y.; Du, X.; Wang, X.; He, J.; Yu, Y.; He, H. *Sens. Actuators B* **2010**, *151*, 205.
- (14) Wang, J.; Yin, S.; Zhang, Q.; Saito, F.; Sato, T. *Solid State Ionics* **2004**, *172*, 191.
- (15) Gombac, V.; De Rogatis, L.; Gasparotto, A.; Vicario, G.; Montini, T.; Barreca, D.; Balducci, G.; Fornasiero, P.; Tondello, E.; Graziani, M. *Chem. Phys.* **2007**, *339*, 111.
- (16) (a) Deluga, G. A.; Salge, J. R.; Schmidt, L. D.; Verykios, X. E. *Science* **2004**, *303*, 993. (b) Huber, G. W.; Dumesic, J. A. *Catal. Today* **2006**, *111*, 119. (c) Huber, G. W.; Shabaker, J. W.; Dumesic, J. A. *Science* **2003**, *300*, 2075.
- (17) Arora, M. K.; Sinha, A. S. K.; Upadhyay, S. N. *Ind. Eng. Chem. Res.* **1998**, *37*, 3950.
- (18) Boumaza, S.; Bouarab, R.; Trari, M.; Bouguelia, A. *Energy Convers. Manage.* **2009**, *50*, 62.
- (19) Hu, L.; Peng, Q.; Li, Y. *J. Am. Chem. Soc.* **2008**, *130*, 16136.
- (20) Ma, C. Y.; Mu, Z.; Li, J. J.; Jin, Y. G.; Cheng, J.; Lu, G. Q.; Hao, Z. P.; Qiao, S. Z. *J. Am. Chem. Soc.* **2010**, *132*, 2608.
- (21) Barreca, D.; Gasparotto, A.; Lebedev, O. I.; Maccato, C.; Pozza, A.; Tondello, E.; Turner, S.; Van Tendeloo, G. *CrystEngComm* **2010**, *12*, 2185.
- (22) Barreca, D.; Massignan, C.; Daolio, S.; Fabrizio, M.; Piccirillo, C.; Armelao, L.; Tondello, E. *Chem. Mater.* **2001**, *13*, 588.
- (23) Hu, Y.-S.; Kleiman-Shwarstein, A.; Stucky, G. D.; McFarland, E. W. *Chem. Commun.* **2009**, 2652.
- (24) Murphy, A. B. *Sol. Energy Mater. Sol. Cells* **2007**, *91*, 1326.
- (25) Zolfaghari, A.; Nasiri Avanki, K.; Jooya, H. Z.; Sayahi, H. *Semicond. Sci. Technol.* **2007**, *22*, 653.
- (26) Chen, J.; Ollis, D. F.; Rulkens, W. H.; Bruning, H. *Water Res.* **1999**, *33*, 669.
- (27) Syu, M. J. *Appl. Microbiol. Biotechnol.* **2001**, *55*, 10.
- (28) Xiu, Z.-L.; Zeng, A.-P. *Appl. Microbiol. Biotechnol.* **2008**, *78*, 917.
- (29) Oh, Y.-C.; Jenks, W. S. *J. Photochem. Photobiol., A* **2004**, *162*, 323.
- (30) Minero, C.; Mariella, G.; Maurino, V.; Vione, D.; Pelizzetti, E. *Langmuir* **2000**, *16*, 8964.
- (31) Montoya, J. F.; Salvador, P. *Appl. Catal., B* **2010**, *94*, 97.
- (32) Yu, J. C.; Yu, J.; Ho, W.; Jiang, Z.; Zhang, L. *Chem. Mater.* **2002**, *14*, 3808.
- (33) Kondarides, D. I.; Patsoura, A.; Verykios, X. E. *J. Adv. Ox. Technol.* **2010**, *13*, 116.